HiPSC-Derived NSCs Effectively Promote The Functional Recovery of Acute Spinal Cord Injury in Mice

Desheng Kong
hebei medical university
Baofeng Feng
Hebei Medical University
Asiamah Ernest Amponsah
Hebei Medical University
Jingjing He
hebei medical university
Ruiyun Guo
hebei medical university
Boxin Liu
hebei medical university
Xiaofeng Du
Hebei Medical University
Xin Liu
Hebei Medical University
Shuhan Zhang
hebei medical university
Fei Lv
hebei medical university
Jun Ma (junmahmu@163.com)
Hebei Medical University https://orcid.org/0000-0003-2843-0769
Huixian Cui
hebei medical university

Research

Keywords: spinal cord injury, induced pluripotent stem cell, neural stem cell, mesenchymal stem cell

Posted Date: November 11th, 2020

DOI: https://doi.org/10.21203/rs.3.rs-102947/v1

Version of Record: A version of this preprint was published on March 11th, 2021. See the published version at https://doi.org/10.1186/s13287-021-02217-9.

Abstract

Background: Spinal cord injury (SCI) is a common disease that results in motor and sensory disorders and even lifelong paralysis. The transplantation of stem cells, such as embryonic stem cells (ESCs), induced pluripotent stem cells (iPSCs), mesenchymal stem cells (MSCs), or subsequently generated stem/progenitor cells, is predicted to be a promising treatment for SCI. In this study, we aimed to investigate effect of human iPSC-derived neural stem cells (hiPSC-NSCs) and umbilical cord-derived MSCs (huMSCs) in a mouse model of acute SCI.

Methods: Acute SCI mice model were established and were randomly treated as PBS (control group), repaired with 1×10^5 hiPSC-NSCs (NSC group), and 1×10^5 huMSCs (MSC group), respectively, in a total of 54 mice (n = 18 each). Hind limb motor function was evaluated in open-field tests using the Basso Mouse Scale (BMS) at days post-operation (dpo) 1, 3, 5 and 7 after spinal cord injury, and weekly thereafter. Spinal cord and serum samples were harvested at dpo 7, 14 and 21. HE staining and Masson staining were used to evaluate the morphological changes and fibrosis area. The differentiation of the transplanted cells in vivo was evaluated with immunohistochemical staining.

Results: The hiPSC-NSC-treated group presented a significantly smaller GFAP+ area than MSC-treated mice at all time points. Additionally, MSC-transplanted mice had a similar GFAP+ area to mice receiving PBS. At dpo14, the immunostained hiPSC-NSCs were positive for SOX2. Furthermore, the transplanted hiPSC-NSCs differentiated into glial fibrillary acidic protein (GFAP)-positive astrocytes and beta-III tubulin-positive neurons, whereas the transplanted huMSCs differentiated into GFAP-positive astrocytes. In addition, hiPSC-NSC transplantation reduced fibrosis formation and the inflammation level. Compared with the control or huMSC transplanted group, the group with transplantation of hiPSC-NSCs exhibited significantly improved behaviours, particularly limb coordination.

Conclusions: HiPSC-NSCs promote functional recovery in mice with acute SCI by replacing missing neurons and attenuating fibrosis, glial scar formation, and inflammation.

Background

Spinal cord injury (SCI) is a common disease that potentially results in the devastating and permanent loss of neurological function due to the failure of axonal regeneration after injury, thereby interrupting the connection between the brain and the body. Based on the available evidence, the incidence of SCI has increased dramatically during the past decade in China, mainly due to an increase in spinal trauma caused by motor vehicle crashes and falls[1]. The Global Burden of Diseases, Injuries, and Risk Factors Study reported 0.93 million (95% uncertainty interval [UI] 0.78–1.16 million) new cases of SCI, and SCI caused 9.5 million (95% UI 6.7–12.4 million) years of life lived with disability in 2016[2, 3]. Due to the lack of a gold standard or effective treatment, the real challenge facing scientists is an appropriate therapy.

According to numerous preclinical studies, stem cell therapy holds great promise for the treatment of central nervous system (CNS) injuries. The administration of stem cells after traumatic SCI reduces

neuronal loss and improves functional recovery in animal models[4–7]. Two desirable objectives of cell-based therapies are to induce trophic reactions (such as the production of extracellular matrix and diffusible growth factors) and to replace cells lost through injury or disease with transplant-derived cells (such as new oligodendrocytes and neurons) that will enhance the regenerative responses of the host CNS. Trophic factors secreted from transplanted cells have been shown to support neuronal survival and neurite outgrowth.

Mesenchymal stem cells (MSCs) have also attracted attention in cell-based therapy because they are easy to isolate in primary cultures and preserve, raise no ethical concerns and are unlikely to develop into tumours. Additionally, cross-reactivity is minimal or absent[8]. MSCs contribute to reducing the size of the spinal cord injury cavity in rat models of both mild and severe SCI while differentiating into glial fibrillary acidic protein (GFAP)-positive astrocytes and neuronal cells[9]. However, MSCs have also been shown to differentiate into oligodendrocytes, but not into cells expressing neuronal markers (NeuN)[10].

Neural stem cells (NSCs) hold promising therapeutic potential; they exert their therapeutic effect by modulating several supportive functions, including anti-inflammation, remyelination, neuroprotection, and promotion of neurite outgrowth[11]. Following the transplantation of NSCs together with the scaffold “fibrin matrices” into a mouse model of severe SCI, the NSCs differentiated into neurons that supported the formation of electrophysiological relays across sites of complete spinal transection, resulting in functional recovery[12].

Few studies have compared the efficacy of NSC and MSC treatments for SCI[13, 14]; therefore, we generated MSCs from the human umbilical cord (huMSCs) and derived NSCs from hiPSCs (hiPSC-NSCs), and transplanted NSCs or MSCs into SCI mice in this study. The purpose was to examine whether the transplanted NSCs or MSCs promoted functional recovery of the hind limbs by attenuating or preventing inflammation and glial scarring and to explore whether hiPSC-NSCs or huMSCs represent a potential treatment for spinal cord injury.

Materials And Methods

2.1 Ethics statement

The collection of all human samples and the performance of animal studies were approved by the Committee of Ethics on Experimentation of Hebei Medical University (Assurance No. 20190505). The experiments were conducted in accordance with the National Institutes of Health Guidelines for the Care and Use of Laboratory Animals.

2.2 Harvesting iPSC-derived NSCs

The hiPSCs were generated from dermal fibroblasts using a protocol previously described in a study from our lab (Cell line: HEBHMUi002-A)[15]. Briefly, fibroblasts at passage 4 were reprogrammed into hiPSCs using the Cytotune™-iPS 2.0 Sendai Reprogramming kit (Thermo Fisher Scientific, Waltham, MA, USA)

according to the manufacturer's guideline. On day 0 of transduction, 4 reprogramming factors were added to fibroblasts, and the medium was changed 24 h later to remove the virus. On day 7 post-transduction, the cells were transferred to a 6-well plate coated with Geltrex hESC-qualified Basement Membrane Matrix (Thermo Fisher Scientific, Waltham, MA, USA) at the recommended density. After 24 h, the medium was changed to Essential 8™ Medium (Gibco, Grand Island, NY, USA); hiPSC colonies were ready to be manually picked an average of 14 days after transduction and characterized using standard validated methods.

We used the PSC Neural Induction Medium (Gibco) to induce iPSCs to become NSCs according to the recommended protocol. Briefly, iPSCs were cultured in the PSC neural induction medium [Neurobasal® Medium (Gibco) supplemented with 10% Neural Induction Supplement (Gibco)] on a Geltrex-coated 6-well-plate, and the medium was changed every other day. After 7 days, the iPSCs differentiated into neural stem cells[15, 16]. The derived cells were fixed with 4% paraformaldehyde (Sigma, St. Louis, MO, USA) in DPBS (Invitrogen, Carlsbad, CA, USA) for immunofluorescence staining (Nestin, SOX2, PAX6, and OCT4: Abcam, Cambridge, UK,detail information in Addational file 1: Table. S1).

2.3 huMSC culture and characteristics

Human umbilical cords were obtained from full-term neonates after caesarean section at the Second Hospital of Hebei Medical University (Shijiazhuang, China). The patients had been informed a priori and had consented to donate the umbilical cords. The huMSCs were obtained by tissue mass culture. Briefly, under sterile conditions, the cord was cut into 3–4 cm pieces and placed on a dish containing saline solution; each section was cut along the umbilical vein and the outer membrane, venous and arterial walls were gently removed. The residual tissue was cut into 1 mm^3 slices with scissors and fixed evenly at bottom of the culture dish. Complete MSC growth medium with supplement (Jingmeng, Beijing, China) was added to each dish at a volume that covered the bottom of the dish with a thin layer, and placed in a 37°C, 5% CO_2 incubator. Seventeen days later, cell growth was observed; the cells were passaged when they reached approximately 90% confluence. Passage 3–5 cells were used to detect the levels of the surface antigens CD29, CD44, CD73, CD90, CD105, CD 45, and HLA-DR with flow cytometry. Fat induction, bone formation and chondrocyte differentiation experiments were performed with the appropriate differentiation medium (Cyagen, Suzhou, China). Oil Red O staining, Alizarin Red staining and Safranin O staining were used for specific staining.

2.4 Establishment of the SCI model and stem cell transplantation

Eight-week-old female immunodeficient BALB/c nude mice (19–22 g, n = 54) were anaesthetized with an intraperitoneal injection of 1% pentobarbital sodium (50 mg/kg, i.p. Hubei XinRunde Chemical Co., Ltd, Wuhan, China). A laminectomy was performed at the 10th thoracic vertebra to expose the dorsal surface of the spinal dura mater. A contusive SCI was induced at the level of T10 using a Zhongshi impactor with weight of 10 g and height of 5 cm (Zhongshi, Beijing, China). In the NSC group, 1×10^5 hiPSC-NSCs/μl were transplanted into the injured spinal cord (1 mm rostral to the lesion epicentre) of 18 mice using a

glass pipette at a rate of 0.5 µl/minute with a 10-µl Hamilton syringe and a stereotaxic microinjector (RWD, Shenzhen, China). Using the same method, eighteen mice were injected with 1×10^5 huMSCs/µl (MSC group), and 18 mice were injected with 1 µl of PBS (control group). All surgeries were conducted under anaesthesia, and efforts were made to minimize the animals' suffering, with selected humane endpoints.

2.5 Behavioural test of locomotor function

Hind limb motor function was evaluated in open-field tests using the Basso Mouse Scale (BMS)[17] at days post-operation (dpo) 1, 3, 5 and 7 after spinal cord injury, and weekly thereafter. Mice were placed on a flat surface with dimensions of 20 cm × 40 cm and observed for 3 min. Two observers who were blinded to the groups simultaneously evaluated the animals' behaviours. A score of 0 represents flaccid paralysis; a score of 9 represents normal gait. For the stepping score, 0 indicates no stepping, and scores of 1, 2, and 3 indicating occasional, frequent and consistent dorsal stepping with no plantar stepping, respectively. Scores of 4, 5, and 6 represent occasional, frequent and consistent plantar stepping, respectively.

2.6 Histology and immunofluorescence staining

Mice were terminally anaesthetized, perfused with saline, then perfused with 4% paraformaldehyde (PFA) in PBS for fixation. The spinal cord was removed from the body, maintained overnight in 4% PFA (4 ℃) then cryoprotected overnight in 30% sucrose in PBS. On the next day, the spinal cord was trimmed to the injured portion (5 mm of the total length), embedded in Tissue-Tek compound (Wetzlar, Germany), frozen and maintained at − 80 ℃. Tissue sections with a thickness of 14 µm were obtained for haematoxylin-eosin staining (H&E) and Masson's trichrome staining.

A primary antibody directed against human nuclei (HuNu, human nuclei antibody, Gene Tex, Irvine, CA, USA) was used to identify human cells transplanted into the mouse spinal cord. Antibodies against GFAP (Thermo Fisher Scientific), beta III Tubulin (TUJ-1, Abcam, Cambridge, MA, UK) and SOX2 (Abcam, Cambridge, MA, UK) were used to follow the fate of the transplanted stem cells and their interaction with the host tissue. Frozen sections were permeabilized in 0.1% Triton X-100 for 20 min. Non-specific protein binding was blocked by incubating the sections with 5% goat serum in PBS for 30 min, followed by an incubation with the primary antibody solution. After an overnight incubation at 4 °C, the sections were successively washed twice with 0.05% PBS-Tween followed by PBS for 5 min each. Sections were then incubated with a DyLight 594-conjugated secondary goat anti-mouse IgG (H + L) antibody and FITC-conjugated goat anti-rabbit IgG (H + L) antibody (Thermo Fisher Scientific) for 1 h at room temperature. Nuclei were counterstained with 4,6-diamidino-2-phenylindole (DAPI, Cell Signalling, Danvers, MA, USA).

2.7 Measurement of serum cytokine levels

The serum levels of cytokines were measured to assess the effects of the transplantation of various stem cells (huMSCs and hiPSC-NSC) on inflammation at 7, 14, and 28 days after SCI (n = 6 animals from each group per time point). The blood was collected, incubated overnight at 4 ℃, and centrifuged at 5000 rpm,

after which the sera were collected for ELISAs to measure the cytokines. ELISAs for VEGF, IL-6, and TNF-α were performed using mouse ELISA kits (Abconal, Wuhan, China) according to the manufacturer's instructions. The OD value at 450 nm (reference at 570 nm) was detected with SPARK (Tecan Trading AG, Switzerland), and the absolute concentration was calculated from the standard curve.

2.8 Quantitative analysis

Four high power (× 200) fields in each section stained with Masson's trichrome were selected to calculate the ratio of the fibrotic area of the spinal cord to the whole area using Image-Pro Plus 6.0 software (Media Cybernetics, Silver Spring, MD, USA)[18]. The intensity of immunofluorescence staining for GFAP was quantified by measuring the integrated optical density (IOD) using Image-Pro Plus 6.0 software, as described in a previous report[19]. Briefly, the glial scar area was quantified by measuring the area of dense GFAP staining near the injury epicentre and excluding the lesion, as defined by absence of GFAP staining, using a 150 μm grid. The average GFAP staining intensity was obtained.

2.9 Statistical Analysis

All quantitative data are reported as the means ± standard errors of the means (SEM) and were analysed using the SPSS 22.0 (StatSoft, Tulsa, OK, USA) or GraphPad PRISM 7.0 (GraphPad Software, San Diego, USA) statistical packages. The statistical significance of differences between the three groups was evaluated using one-way ANOVA, while Tukey's multiple comparisons test was used as a post hoc analysis to assess differences between any two groups. Statistical significance was set to $p < 0.05$.

Results

3.1 The characterization of hiPSC-NSCs and huMSCs

The hiPSC-NSCs that were derived from hiPSCs expressed the markers Nestin, SOX2, and PAX6 (Fig. 1A). Flow cytometry and induced differentiation were performed to characterize the huMSCs. As shown in Fig. 1B, the huMSCs were positive for specific MSC surface markers, including CD29, CD44, CD73, CD90 and CD105, and negative for CD45 and HLA-DR (Fig. 1B). The huMSCs were capable of adipogenic, osteogenic, and chondrogenic differentiation as determined by the results of Oil Red O, Alizarin Red S, and Alcian Blue staining, respectively (Fig. 1C).

3.2 Pathomorphological changes

A cavity formed in the injured spinal cord of the PBS group, and the surface of the injured spinal cord was collapsed. The surface of the injured spinal cord in the NSC group was plump, smooth, and not significantly collapsed. At dpo 28, numerous inflammatory cells and fibroblasts had infiltrated the SCI site in the PBS group. The MSC group exhibited a lower level of inflammatory cell infiltration than the PBS group, and a reduced area of necrotic tissue. The SCI site of the NSC group spanned a smaller area than the other two groups (Fig. 2). The percentage of fibrosis at the SCI site was evaluated to assess recovery and scar formation. At all time points, the smallest fibrotic area was observed in the NSC group among

the three groups, although the differences were not significant at dpo 7 and dpo 14. A significantly lower average percentage of fibrosis was observed in the NSC group than in the control group [(23.33 ± 2.03)% *vs.* (64.48 ± 3.10)%, $p < 0.001$] and the percentage of fibrosis was significantly decreased in the MSC group compared with the control group [(32.51 ± 3.51)% *vs.* (64.48 ± 3.10)%, $p < 0.001$)].

3.3 Astrogliosis following Stem Cell Transplantation

Anti-GFAP immunostaining was performed to assess the distribution of astrocytes and formation of a glial scar at dpo 7, 14 and 28 after the contusion (Fig. 3A-C). Astrocytes were packed tightly and formed a scar barrier in the control group. However, in the NSC group, the astrocytes appeared to be permissive and did not form a prominent glial limitans to completely block regenerating axons (Fig. 3B). As expected, the lesion in the NSC group showed significantly less GFAP-positive glial scarring. In contrast, a massive glial scar was observed in the MSC group, with no significant difference from the control group (Fig. 3). The quantitative analysis showed a significant decrease in GFAP expression in the NSC group compared with the control and MSC groups at dpo 7 and 14. Moreover, GFAP expression showed a decreasing trend in the control and MSC groups, while its expression was slightly increased in the NSC group. The hiPSC-NSC-treated group presented a significantly smaller GFAP + area than MSC-treated mice at all time points. Additionally, MSC-transplanted mice had a similar GFAP + area to mice receiving PBS (Fig. 5A).

3.4 The fate and directional differentiation of transplanted cells

The surviving stem cells were stained with HuNu (Fig. 4A-C). Differentiation of the transplanted stem cells in the injured spinal cord of the three stem cell transplanted groups was identified using cell marker antibodies, and the PBS group was used as the negative control group. Cells with HuNu-positive nuclei (red) were observed in the spinal cord sections from the NSC group, and they were double stained with either GFAP or TUJ1 (Fig. 4). Thus, the transplanted cells had differentiated into astrocytes and neurons. Some cells with SOX2-positive nuclei were also observed, indicating that some NSCs were still alive (SOX2-positive cells). Cells with HuNu-positive nuclei (red) were observed in the MSC group and were double stained with the anti-GFAP antibody (green), but were not double-stained with the anti-TUJ1 or anti-SOX2 antibody. In our experiment, the surviving huMSCs in the injured spinal cord differentiated into astrocytes, but not neural cells. No transplanted stem cells were observed in the PBS group.

3.5 The serum cytokine levels in mice with a spinal cord injury

The level of IL-6 in the MSC group at dpo 7 was (45.50 ± 6.26) pg/ml, which was significantly higher than in the other groups [NSC group: (23.63 ± 1.80) pg/ml, control group: (25.57 ± 3.33) pg/ml]. At dpo 14, no differences were observed among the three groups. At dpo 21, the IL-6 level was significantly decreased compared with the level detected at dpo 14 in the NSC group [(13.56 ± 2.77) pg/ml], and a lower level was

observed compared to the levels in the other groups at the same time point (Fig. 5B). VEGF levels in the NSC group decreased gradually as the injury healed. Significantly lower VEGF levels were observed in the NSC group than in the other two groups at dpo 28. In the MSC group, the VEGF level at dpo 28 was significantly higher than at dpo 7. The levels detected in PBS-treated animals remained unchanged at all time points (Fig. 5C). No significant difference in TNF-α levels was detected among three groups at different time points (Fig. 5D).

3.6 Behavioural analysis of locomotor function

The huMSCs, hiPSC-NSC, or PBS in the control group were transplanted by an intramedullary injection into the injured area immediately after spinal cord contusion. After contusion-induced SCI, locomotor function was evaluated with the BMS locomotor rating scale in an open field. Almost complete hind limb paralysis was observed in both groups at dpo 1 (Fig. 6G-I, Addational file 2–4: Videos 1–3), and BMS scores of the three groups were similar (Fig. 6A). The locomotor function gradually improved in the NSC group throughout the observation period, while the function of the MSC group and control group recovered before dpo 14 and then decreased. At dpo 3, the score of NSC group was significantly higher than the scores of the other two groups [(3.11 ± 0.21) *vs.* (2.49 ± 0.17) and (2.19 ± 0.14)]. Similarly, a higher BMS score was recorded for the NSC group at dpo 7 and 14. Interestingly, transplanted animals in the NSC group always showed better maximum scores on the BMS test at shorter times after SCI. At dpo 28, the muscles of the lower limbs and buttocks of mice in the control group and MSC group had obviously atrophied, while the shapes of muscles were approximately normal in the NSC group (Fig. 6G'-I', Addational file 5–7: Videos 4–6). Transplanted animals in the NSC group reached the maximum score (4.71 ± 0.22), which was significantly higher than the scores of the MSC group and control group [(3.18 ± 0.40) and (2.59 ± 0.25), respectively].

The subscores for plantar stepping, coordination, paw position, trunk, and tail were tallied. At dpo 1, the subscore of animals in all groups decreased to zero. At dpo 28, the mean subscore of the NSC group was 1.07, a value that was significantly higher than the other groups (MSC group: 0.35, control group: 0.06) (Fig. 6B). Regarding changes in coordination, by dpo 28, 71% of the NSC-treated mice displayed some or a substantial restoration of coordination compared with 38% of the controls (Fig. 6C). Importantly, 29% of the NSC-treated mice were able to perform a mild trunk dysfunction, in contrast to 0% of the controls and 11% of the MSC group (Fig. 6D). Although the NSC group had a higher stepping score on the left and right sides compared with the MSC and control group, statistically significant differences were not observed among these groups (Fig. 6E-F). Thus, the hiPSC-NSC treatment was highly beneficial for the recovery of systemic function (e.g., coordination and trunk function) in the SCI mice.

Discussion

Spinal cord injury (SCI) is currently the most difficult traumatic neurological condition to treat in the clinic. Following the primary injury, which causes immediate structural damage, a series of secondary injuries, including haemorrhage, enema, demyelination, and axonal and neuronal necrosis, occur[20]. Cell

transplantation is a promising treatment, including NSCs/NPCs[21], MSCs[22], and Schwann cell-like cells[23]. To date, three main sources of NSCs have been described: direct isolation from the primary CNS tissue (either from the foetal or adult brain), differentiation from pluripotent stem cells, and transdifferentiation from somatic cells. Notably, iPSC-derived NSCs have striking advantages over ESC-derived NSCs, namely, the possibility of autologous transplantation[24]. Recent investigations have also examined the utility of MSCs recovered from tissues other than the bone marrow, including the umbilical cord and adipose tissue[25]. In the present study, we transplanted hiPSC-NSCs or huMSCs into the spinal cord following SCI.

The fibrous glial scar formed by infiltrated inflammatory cells (including microglia, fibroblasts, and reactive astrocytes) limits axon regeneration across the lesion[26, 27]. The scar tissue not only exerts a protective effect by limiting the spread of inflammation and secondary damage to adjacent intact tissue but also serves as an inhibitory barrier for axon regeneration[28, 29]. Most studies conducted to date have focused on the glial scar component of the scar tissue, while the fibrotic component has received less attention. In the present study, hiPSC-NSC and huMSC transplantation reduced spinal cord fibrosis. The hiPSC-NSCs were more effective, although the difference between hiPSC-NSCs and huMSCs was not significant. Fibrotic components are not expressed at high levels in the normal adult spinal cord, and previous studies have suggested that the excess deposition observed after SCI might be attributed to various sources, such as reactive astrocytes, macrophages, and fibroblasts[28, 30]. The fibrotic changes among the different groups were similar to changes in the GFAP levels, with the lowest levels observed in the hiPSC-NSC group.

The fate of transplanted cells is determined by the environment into which the cells are transplanted rather than the intrinsic properties of the cells. In our study, allogenic MSCs survived in injured spinal cords and integrated into the host tissue without the requirement for administering immunosuppressive agents. In the present study, the transplanted huMSCs were positive for GFAP immunostaining at dpo 14, thus confirming the differentiation of huMSCs into the astrocytic lineage. The huMSCs have been confirmed to differentiate into CNS cell lineages in a rat SCI model[28, 30, 31]. Some authors investigated BM-MSC transplantation in dogs[32, 33]. Among them, Ryu et al.[32] recorded improved neurological outcomes in MSC groups after acute transplantation (one week after trauma), since all dogs exhibited purposeful hind limb motion. Moreover, some MSCs expressed markers for neurons (NF160), neuronal nuclei (NeuN) and astrocytes (GFAP)[34]. Based on our data, the transplanted hiPSC-NSCs differentiated into neuronal nuclei (NeuN)- and β-tubulin isotype III (β III tubulin)-positive neurons and glial fibrillary acidic protein (GFAP)-positive astrocytes. The most common approach for stem cell transplantation in mouse models is to inject the cells into the epicentre of the injured site. However, the tissue environment of the injured CNS is unfavourable for graft cell survival[35–37]. The number of transplanted cells gradually decreases and cells disappear from the spinal cord 3 weeks after injection[9]. When the NSCs or MSCs were transplanted in the acute phase after injury, the stem cells were no longer detected at dpo 28.

SCI induces an increase in the expression of pro-inflammatory cytokines (TNF-α, IL-6, and IL-1β), while it decreases the expression of the anti-inflammatory cytokine IL-10 [38]. As shown in the study by Cheng et al. [5], the NSC medium was able to suppress the expression of the pro-inflammatory cytokine IL-6. In the present study, NSC transplantation decreased the IL-6 level, which promoted recovery and improved locomotion. However, the level of IL-6 in the MSC group was similar to the control group. In the course of healing from the injury, the VEGF level detected in the NSC group at dpo 28 was lower than at dpo 14. A significant difference in serum TNF-α levels was not observed among the different groups at different time points. In mouse models of SCI, TNF-α-expressing cells were initially observed around the injured site at 30 to 45 min after injury, and TNF-α expression was substantially increased from 3 to 24 hrs[539, 40]. In our study, TNF-α was initially detected at dpo 7, and thus we may have missed the change in its expression. Pro-inflammatory cytokines are released from damaged cells; reactive microglia then recruit immune cells from broken blood vessels and promote tissue repair. Because reactive microglia and recruited macrophages are the main inflammatory cytokine-producing cells, the inflammatory response is then further exacerbated. The administration of IL-6, which is an important trigger of inflammatory cytokine production, to the injured spinal cord causes increased recruitment of neutrophils, an expansion of the areas occupied by macrophages and activated microglia, and reduced axonal regeneration [41, 42]. Therefore, inflammatory cytokines are strongly associated with the secondary damage after SCI.

Immunofluorescence staining showed that hNSCs and huMSCs differentiate into neurons and astrocytes; however, the functional outcome differed between the NSC and the MSC group, and the NSCs produced a better outcome than PBS and MSCs. The results are consistent with the morphological changes. A positive effect of the huMSC treatment on function was observed, but the difference was not statistically significant. The results differed from other studies[43, 44]. These opposing results are potentially attributed to the time of transplantation. Moreover, hiPSC-NSCs promoted functional recovery in SCI-induce mice not only primarily through cell differentiation and direct replacement of the lost cells but also through neuroprotective mechanisms, such as immunomodulatory factors to enhance axonal growth, modulate the environment, and reduce neuroinflammation[13].

Conclusions

Based on our results, hiPSC-NSCs are capable of surviving and differentiating in an injured spinal cord. hiPSC-NSCs reduced the levels of pro-inflammatory cytokines after SCI and hence subsequently alleviated secondary damage, as evidenced by the reductions in glial scar and fibrotic scar formation. Therefore, hiPSC-NSC transplantation for acute SCI promotes the recovery of limb function, indicating that hiPSC-NSCs are a promising cell type for SCI treatment.

Abbreviations

SCI: spinal cord injury; ESCs: embryonic stem cells, iPSCs: induced pluripotent stem cells; MSCs: mesenchymal stem cells; NSCs: neural stem cells; hiPSC-NSCs: human iPSC-derived NSCs; huMSCs:

human umbilical cord mesenchymal stem cells; GFAP: glial fibrillary acidic protein; BMS: Basso Mouse Scale; HuNu: human nuclei; VEGF: vascular endothelial growth factor; IL-6: Interleukin-6; TNF-α: tumor necrosis factor-α.

Declarations

Acknowledgements

Not applicable.

Ethics approval and consent to participate

All human samples and animal studies were approved by the Committee of Ethics on Experimentation of Hebei Medical University (Assurance No. 20190505). The experiments were conducted in accordance with the National Institutes of Health guidelines for the care and use of animals.

Funding

This work was supported by the following grants: High Level talents funding project in Hebei Province (No. B2019005009) to Desheng Kong. The Program of National Natural Science Foundation of China (No.81801278) and General program of Natural Science Foundation of Hebei Province (No.H2019206637) to Jun Ma.

Availability of data and materials

The data that support the findings of this study are available from the corresponding author upon reasonable request.

Authors' contributions

DSK, HXC and JM designed and planned the study. DSK, BFF, AE.Amponsah and JJH performed animal experiment. RYG, BXL, XFD and XL cultured cells. SHZ and FL collected and analyzed data.DSK was a major contributor in writing the manuscript. JM amended the manuscript. All authors read and approved the final manuscript.

Consent for publication

Not applicable.

Competing interests

The authors declare that they have no competing interests.

References

1. Reinhardt J D, Zheng Y, Xu G, et al. People with Spinal Cord Injury in China[J]. American Journal of Physical Medicine & Rehabilitation, 2017,96:S61-S65.
2. Badhiwala J H, Wilson J R, Fehlings M G. Global burden of traumatic brain and spinal cord injury[J]. The Lancet Neurology, 2019,18(1):24-25.
3. James S L, Theadom A, Ellenbogen R G, et al. Global, regional, and national burden of traumatic brain injury and spinal cord injury, 1990–2016: a systematic analysis for the Global Burden of Disease Study 2016[J]. The Lancet Neurology, 2019,18(1):56-87.
4. Marchini A, Raspa A, Pugliese R, et al. Multifunctionalized hydrogels foster hNSC maturation in 3D cultures and neural regeneration in spinal cord injuries[J]. Proceedings of the National Academy of Sciences, 2019,116(15):7483-7492.
5. Cheng Z, Bosco D B, Sun L, et al. Neural Stem Cell-Conditioned Medium Suppresses Inflammation and Promotes Spinal Cord Injury Recovery[J]. Cell Transplantation, 2017,26(3):469-482.
6. Villanova Junior J A, Fracaro L, Rebelatto C L K, et al. Recovery of motricity and micturition after transplantation of mesenchymal stem cells in rats subjected to spinal cord injury[J]. Neuroscience Letters, 2020,734:135134.
7. Wu L, Pan X, Chen H, et al. Repairing and Analgesic Effects of Umbilical Cord Mesenchymal Stem Cell Transplantation in Mice with Spinal Cord Injury[J]. BioMed Research International, 2020,2020:1-10.
8. Cofano F, Boido M, Monticelli M, et al. Mesenchymal Stem Cells for Spinal Cord Injury: Current Options, Limitations, and Future of Cell Therapy[J]. International Journal of Molecular Sciences, 2019,20(11):2698.
9. Ohta M, Suzuki Y, Noda T, et al. Bone marrow stromal cells infused into the cerebrospinal fluid promote functional recovery of the injured rat spinal cord with reduced cavity formation[J]. Exp Neurol, 2004,187(2):266-278.
10. Čížková D, Rosocha J, Vanický I, et al. Transplants of Human Mesenchymal Stem Cells Improve Functional Recovery After Spinal Cord Injury in the Rat[J]. Cellular and Molecular Neurobiology, 2006,26(7-8):1165-1178.
11. Zhu Y, Uezono N, Yasui T, et al. Neural stem cell therapy aiming at better functional recovery after spinal cord injury[J]. Developmental Dynamics, 2018,247(1):75-84.
12. Lu P, Wang Y, Graham L, et al. Long-distance growth and connectivity of neural stem cells after severe spinal cord injury[J]. Cell, 2012,150(6):1264-1273.
13. Sun L, Wang F, Chen H, et al. Co-Transplantation of Human Umbilical Cord Mesenchymal Stem Cells and Human Neural Stem Cells Improves the Outcome in Rats with Spinal Cord Injury[J]. Cell Transplantation, 2019,28(7):893-906.
14. Park D Y, Mayle R E, Smith R L, et al. Combined Transplantation of Human Neuronal and Mesenchymal Stem Cells following Spinal Cord Injury[J]. Global Spine Journal, 2013,3(1):1-5.
15. Ma J, Zhang J, He J, et al. Induced pluripotent stem cell (iPSC) line (HEBHMUi002-A) from a healthy female individual and neural differentiation[J]. Stem Cell Res, 2020,42:101669.

16. O'Brien L C, Keeney P M, Bennett J J. Differentiation of Human Neural Stem Cells into Motor Neurons Stimulates Mitochondrial Biogenesis and Decreases Glycolytic Flux[J]. Stem Cells Dev, 2015,24(17):1984-1994.
17. Basso D M, Fisher L C, Anderson A J, et al. Basso Mouse Scale for Locomotion Detects Differences in Recovery after Spinal Cord Injury in Five Common Mouse Strains[J]. Journal of Neurotrauma, 2006,23(5):635-659.
18. Kong D, Zhang L, Xu X, et al. Small Intestine Submucosa Is a Potential Material for Intrauterine Adhesions Treatment in a Rat Model[J]. Gynecol Obstet Invest, 2018,83(5):499-507.
19. Salazar D L, Uchida N, Hamers F P, et al. Human neural stem cells differentiate and promote locomotor recovery in an early chronic spinal cord injury NOD-scid mouse model[J]. PLoS One, 2010,5(8):e12272.
20. Steuer I, Guertin P A. Central pattern generators in the brainstem and spinal cord: an overview of basic principles, similarities and differences[J]. Reviews in the neurosciences, 2019,30(2):107-164.
21. Kajikawa K, Imaizumi K, Shinozaki M, et al. Cell therapy for spinal cord injury by using human iPSC-derived region-specific neural progenitor cells[J]. Mol Brain, 2020,13(1):120.
22. Liu A M, Chen B L, Yu L T, et al. Human adipose tissue- and umbilical cord-derived stem cells: which is a better alternative to treat spinal cord injury?[J]. Neural Regen Res, 2020,15(12):2306-2317.
23. Hopf A, Schaefer D J, Kalbermatten D F, et al. Schwann Cell-Like Cells: Origin and Usability for Repair and Regeneration of the Peripheral and Central Nervous System[J]. Cells, 2020,9(9).
24. Pereira I M, Marote A, Salgado A J, et al. Filling the Gap: Neural Stem Cells as A Promising Therapy for Spinal Cord Injury[J]. Pharmaceuticals (Basel, Switzerland), 2019,12(2):65.
25. Jin M C, Medress Z A, Azad T D, et al. Stem cell therapies for acute spinal cord injury in humans: a review[J]. Neurosurg Focus, 2019,46(3):E10.
26. Shao A, Tu S, Lu J, et al. Crosstalk between stem cell and spinal cord injury: pathophysiology and treatment strategies[J]. Stem cell research & therapy, 2019,10(1):213-238.
27. Donnelly D J, Popovich P G. Inflammation and its role in neuroprotection, axonal regeneration and functional recovery after spinal cord injury[J]. Exp Neurol, 2008,209(2):378-388.
28. Zhu Y, Soderblom C, Trojanowsky M, et al. Fibronectin Matrix Assembly after Spinal Cord Injury[J]. Journal of Neurotrauma, 2015,32(15):1158-1167.
29. Shearer M C, Fawcett J W. The astrocyte/meningeal cell interface – a barrier to successful nerve regeneration?[J]. Cell and Tissue Research, 2001,305(2):267-273.
30. Wang W, Tang S, Li H, et al. MicroRNA-21a-5p promotes fibrosis in spinal fibroblasts after mechanical trauma[J]. Experimental cell research, 2018,370(1):24-30.
31. Kuh S U, Cho Y E, Yoon D H, et al. Functional recovery after human umbilical cord blood cells transplantation with brain-derived neutrophic factor into the spinal cord injured rat[J]. Acta Neurochir (Wien), 2005,147(9):985-992, 992.

32. Ryu H, Kang B, Park S, et al. Comparison of mesenchymal stem cells derived from fat, bone marrow, Wharton's jelly, and umbilical cord blood for treating spinal cord injuries in dogs[J]. The Journal of veterinary medical science, 2012,74(12):1617-1630.
33. Khan I U, Yoon Y, Kim A, et al. Improved Healing after the Co-Transplantation of HO-1 and BDNF Overexpressed Mesenchymal Stem Cells in the Subacute Spinal Cord Injury of Dogs[J]. Cell transplantation, 2018,27(7):1140-1153.
34. Nori S, Okada Y, Yasuda A, et al. Grafted human-induced pluripotent stem-cell-derived neurospheres promote motor functional recovery after spinal cord injury in mice[J]. Proceedings of the National Academy of Sciences, 2011,108(40):16825-16830.
35. Fujimoto Y, Abematsu M, Falk A, et al. Treatment of a mouse model of spinal cord injury by transplantation of human induced pluripotent stem cell-derived long-term self-renewing neuroepithelial-like stem cells[J]. Stem Cells, 2012,30(6):1163-1173.
36. Yokota K, Kobayakawa K, Kubota K, et al. Engrafted Neural Stem/Progenitor Cells Promote Functional Recovery through Synapse Reorganization with Spared Host Neurons after Spinal Cord Injury[J]. Stem Cell Reports, 2015,5(2):264-277.
37. Abematsu M, Tsujimura K, Yamano M, et al. Neurons derived from transplanted neural stem cells restore disrupted neuronal circuitry in a mouse model of spinal cord injury[J]. J Clin Invest, 2010,120(9):3255-3266.
38. Kumar H, Choi H, Jo M J, et al. Neutrophil elastase inhibition effectively rescued angiopoietin-1 decrease and inhibits glial scar after spinal cord injury[J]. Acta Neuropathol Commun, 2018,6(1):73.
39. Pineau I, Lacroix S. Proinflammatory cytokine synthesis in the injured mouse spinal cord: multiphasic expression pattern and identification of the cell types involved[J]. J Comp Neurol, 2007,500(2):267-285.
40. Habgood M D, Bye N, Dziegielewska K M, et al. Changes in blood-brain barrier permeability to large and small molecules following traumatic brain injury in mice[J]. Eur J Neurosci, 2007,25(1):231-238.
41. Lacroix S, Chang L, Rose-John S, et al. Delivery of hyper-interleukin-6 to the injured spinal cord increases neutrophil and macrophage infiltration and inhibits axonal growth[J]. J Comp Neurol, 2002,454(3):213-228.
42. Fu E S, Saporta S. Methylprednisolone inhibits production of interleukin-1beta and interleukin-6 in the spinal cord following compression injury in rats[J]. J Neurosurg Anesthesiol, 2005,17(2):82-85.
43. Yang C, Wang G, Ma F, et al. Repeated injections of human umbilical cord blood-derived mesenchymal stem cells significantly promotes functional recovery in rabbits with spinal cord injury of two noncontinuous segments[J]. Stem cell research & therapy, 2018,9(1):136.
44. Li X, Tan J, Xiao Z, et al. Transplantation of hUC-MSCs seeded collagen scaffolds reduces scar formation and promotes functional recovery in canines with chronic spinal cord injury[J]. Scientific reports, 2017,7:43559.

Figures

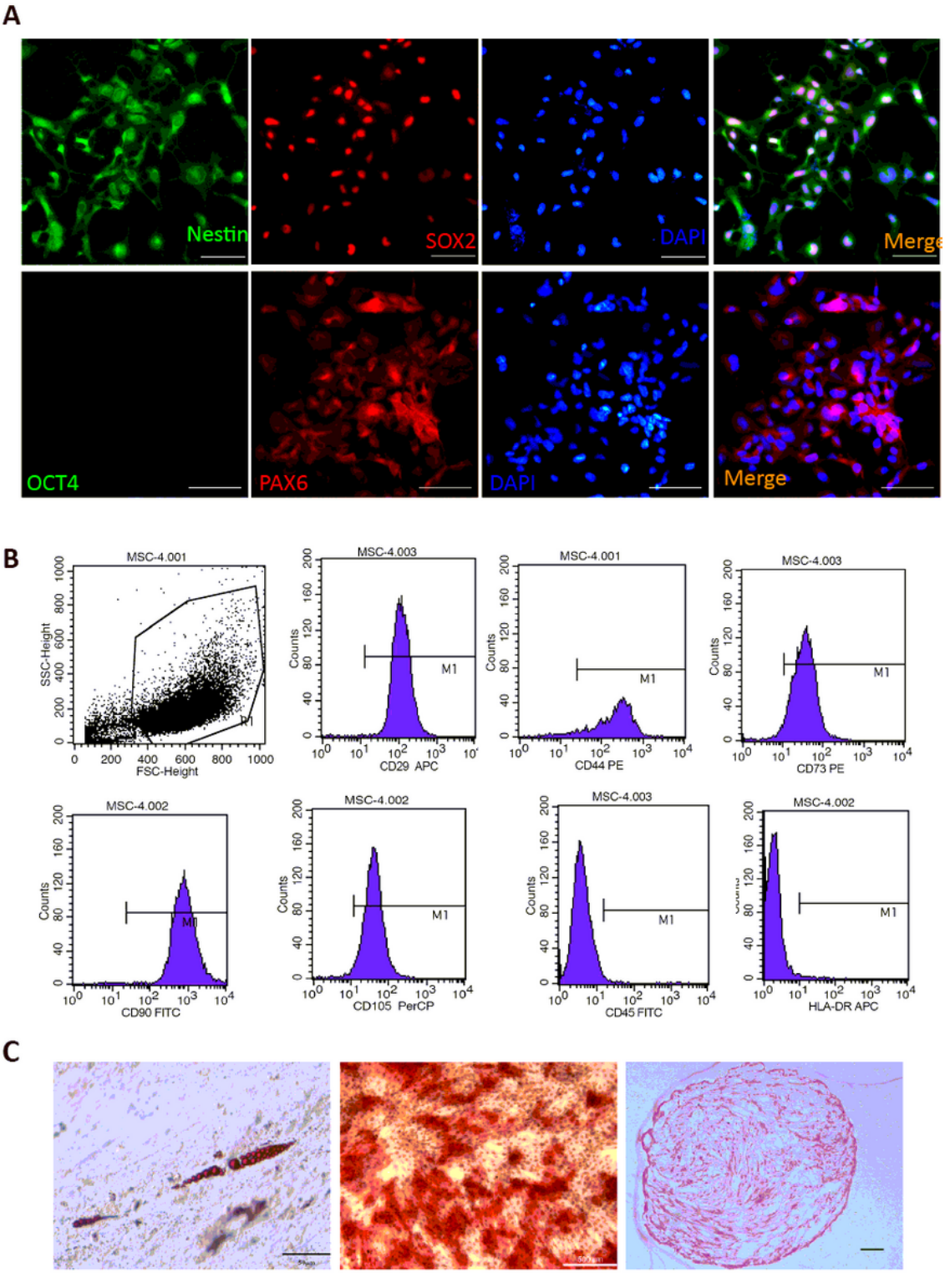

Figure 1

The characteristics of huMSCs. A: Cell surface antigens were detected at passage 4 using flow cytometry. huMSCs were positive for CD29, CD44, CD73, CD90, and CD105. In contrast, very little expression of the haematopoietic lineage markers HLA-DR and CD45 was detected in huMSCs. B: Oil red O staining of lipid droplets revealed that huMSCs differentiated into cells of the adipogenic lineage. Bar: 50 μm. C: Alizarin red staining revealed a calcified extracellular matrix of induced huMSCs, confirming that huMSCs

differentiated into osteogenic cells. Bar: 500 μm. D: Safranin O staining showed the secretion of the extracellular matrix of chondrocytes.

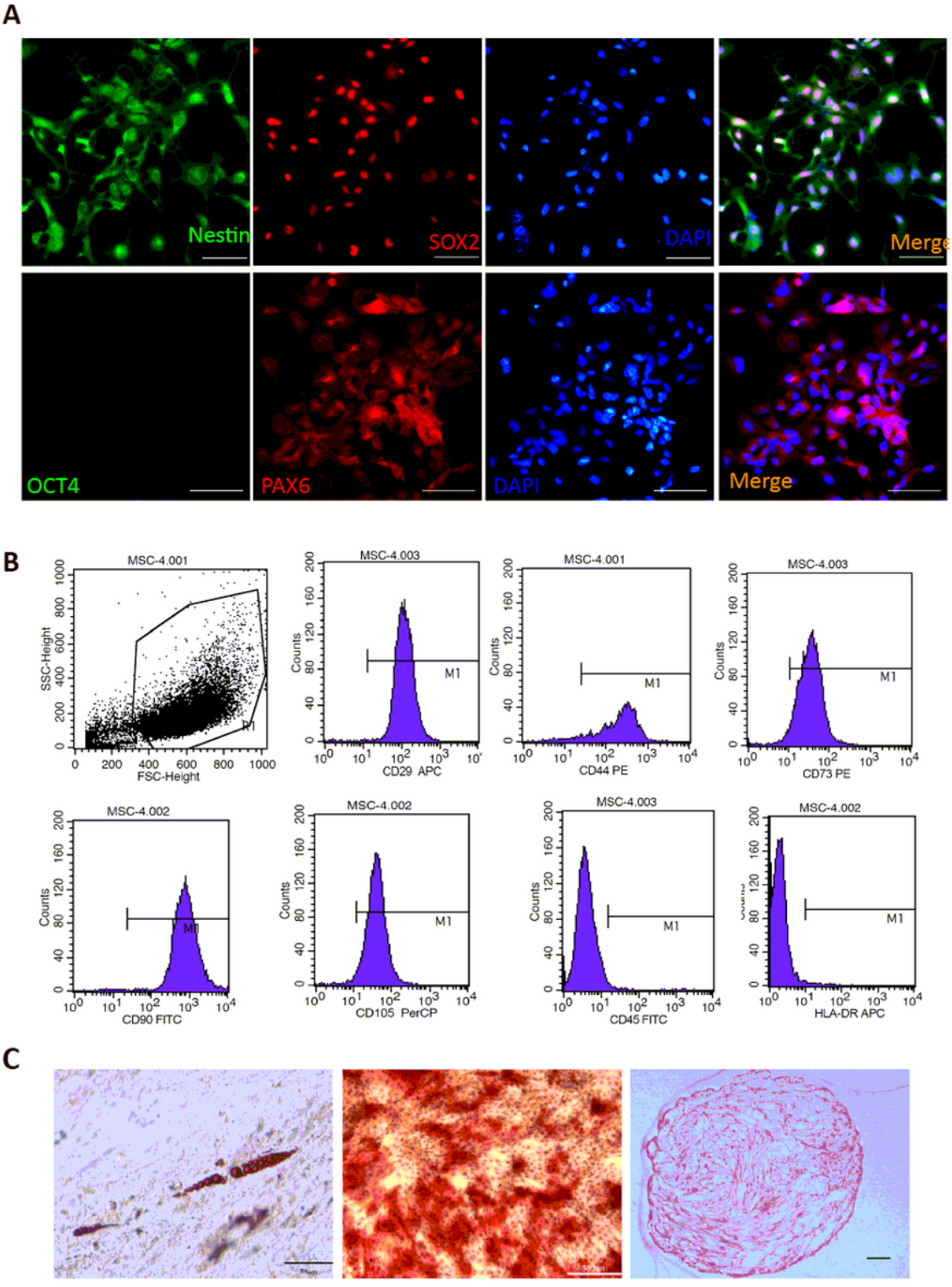

Figure 1

The characteristics of huMSCs. A: Cell surface antigens were detected at passage 4 using flow cytometry. huMSCs were positive for CD29, CD44, CD73, CD90, and CD105. In contrast, very little expression of the haematopoietic lineage markers HLA-DR and CD45 was detected in huMSCs. B: Oil red O staining of lipid

droplets revealed that huMSCs differentiated into cells of the adipogenic lineage. Bar: 50 μm. C: Alizarin red staining revealed a calcified extracellular matrix of induced huMSCs, confirming that huMSCs differentiated into osteogenic cells. Bar: 500 μm. D: Safranin O staining showed the secretion of the extracellular matrix of chondrocytes.

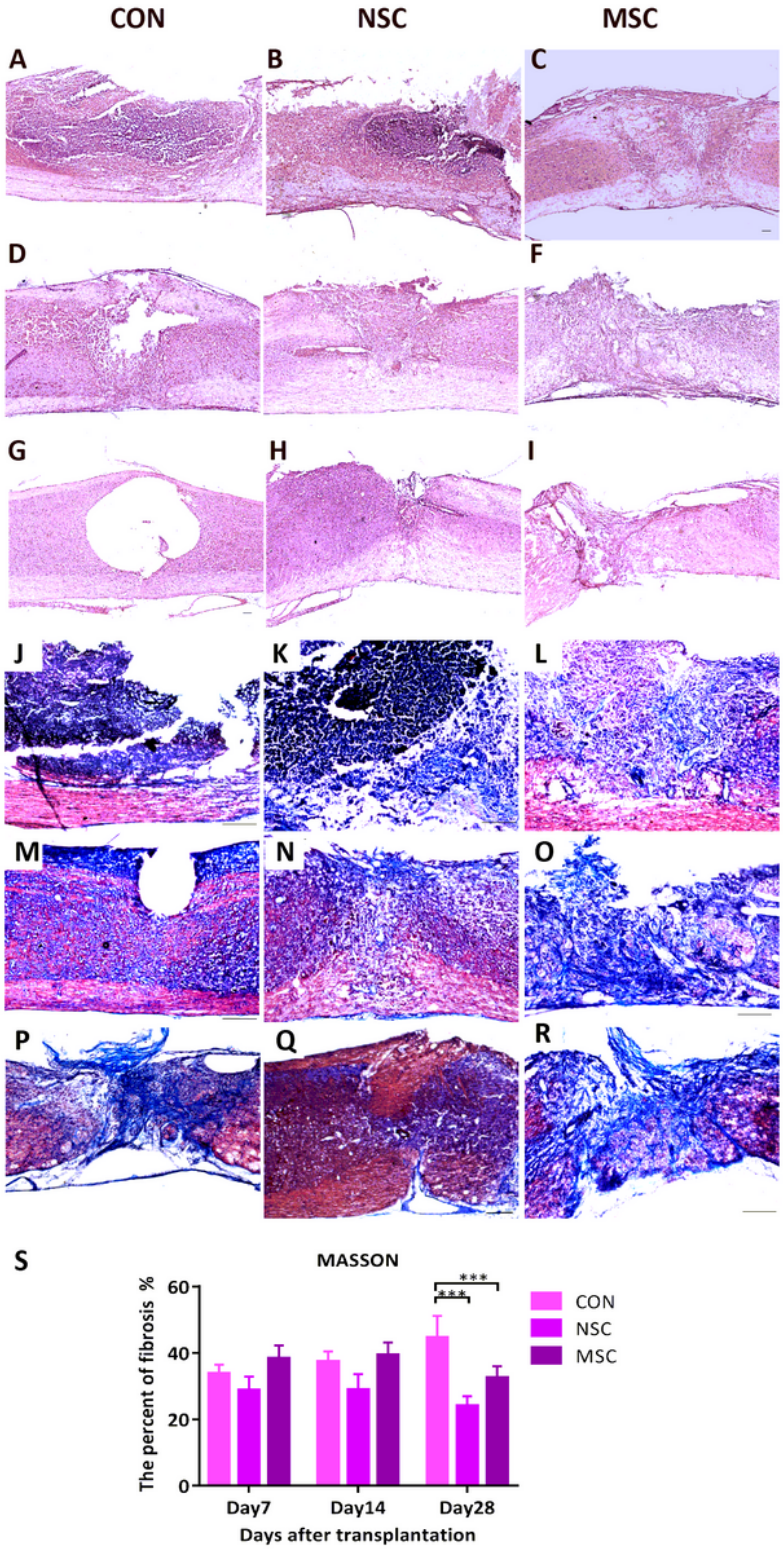

Figure 2

Images of HE staining and Masson's trichrome staining in the different groups at dpo 7(A-C and J-L), dpo14 (D-F and M-O) and dpo28 (G-I and P-R). The percentage of fibrosis in the NSC and MSC groups was significantly lower than in the Control group (S). Scale bar:100 μm.

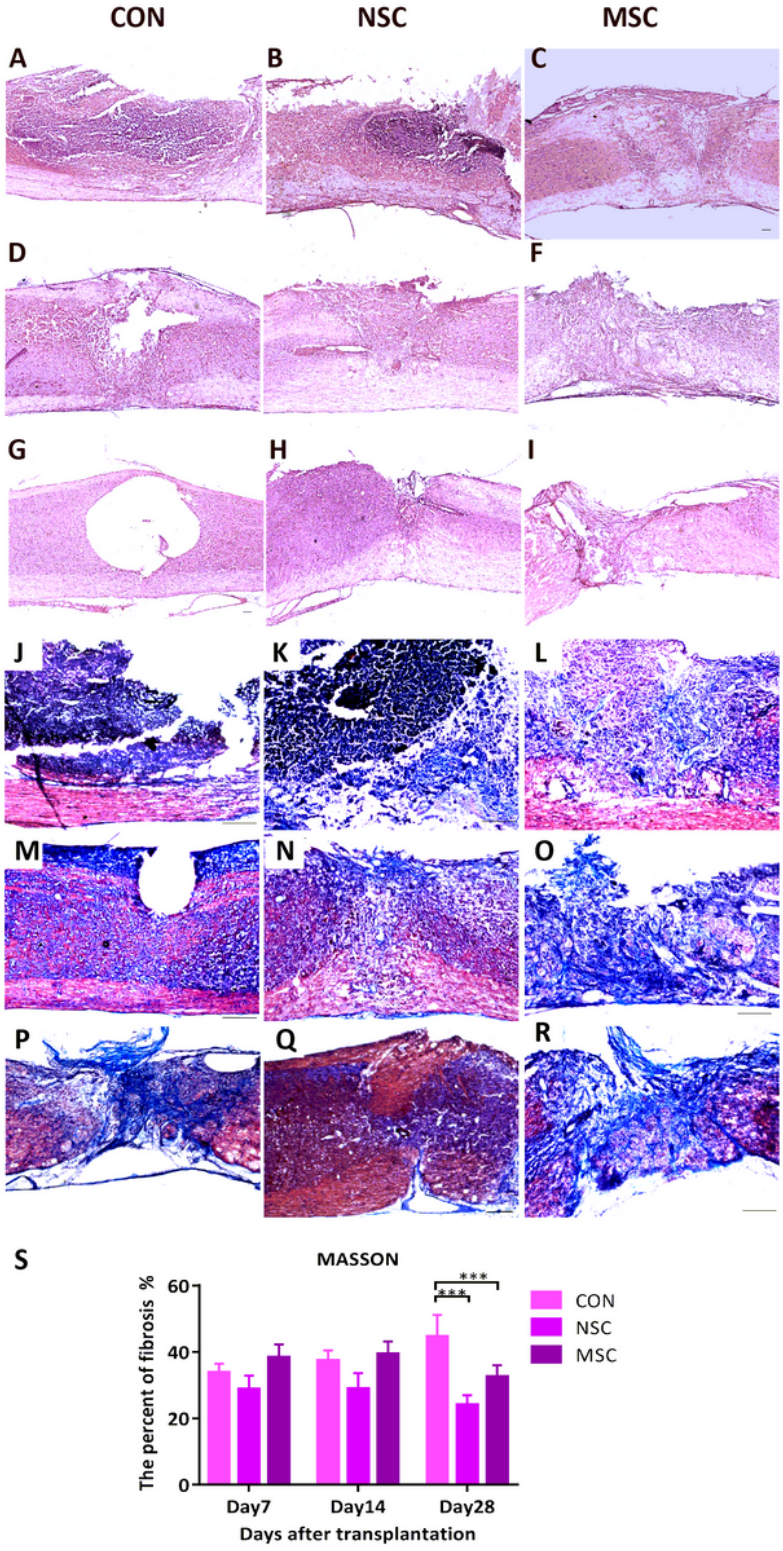

Figure 2

Images of HE staining and Masson's trichrome staining in the different groups at dpo 7(A-C and J-L), dpo14 (D-F and M-O) and dpo28 (G-I and P-R). The percentage of fibrosis in the NSC and MSC groups

was significantly lower than in the Control group (S). Scale bar:100 μm.

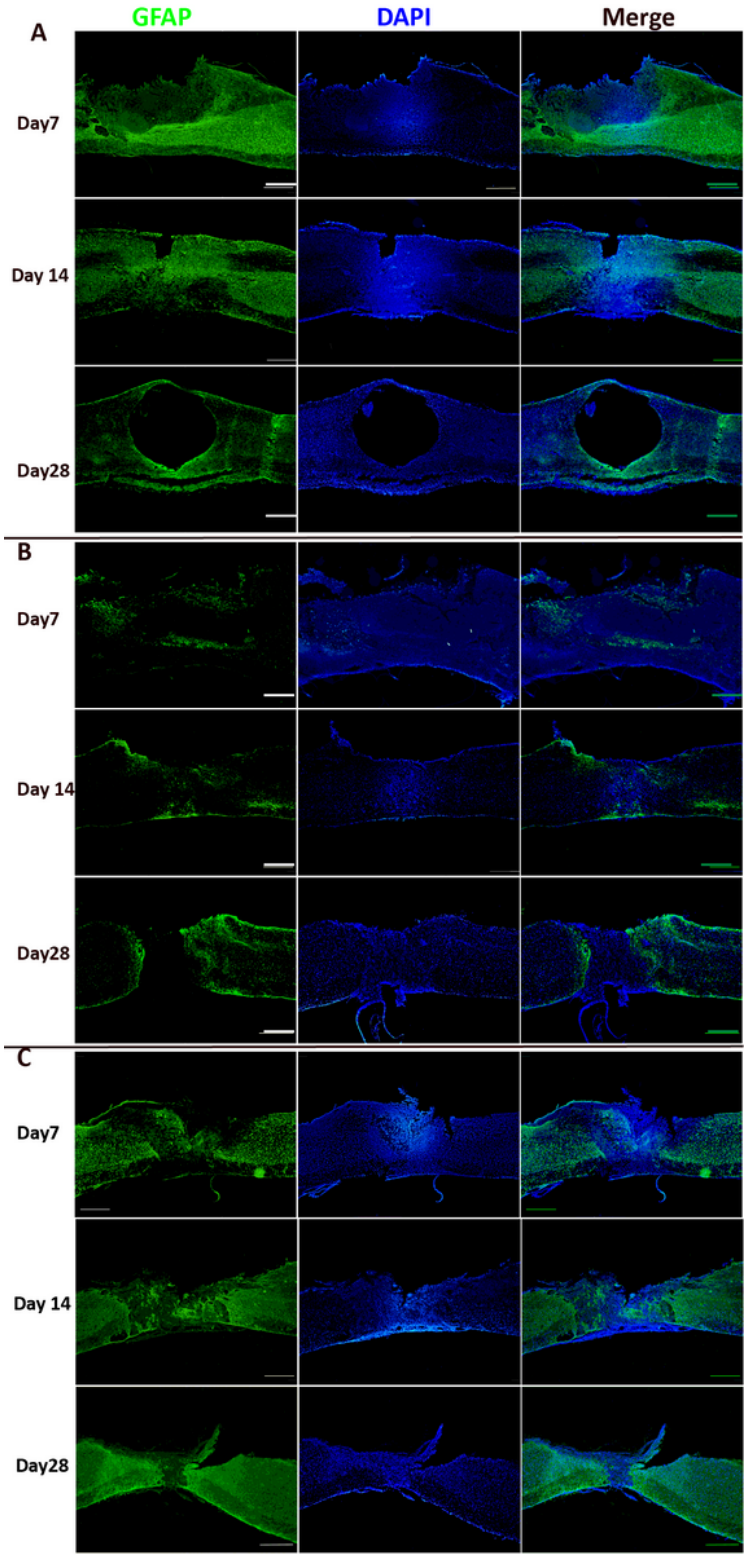

Figure 3

Longitudinal spinal cord sections (14 μm) were immunostained for GFAP to detect astrogliosis. Scale bar: 500 μm.

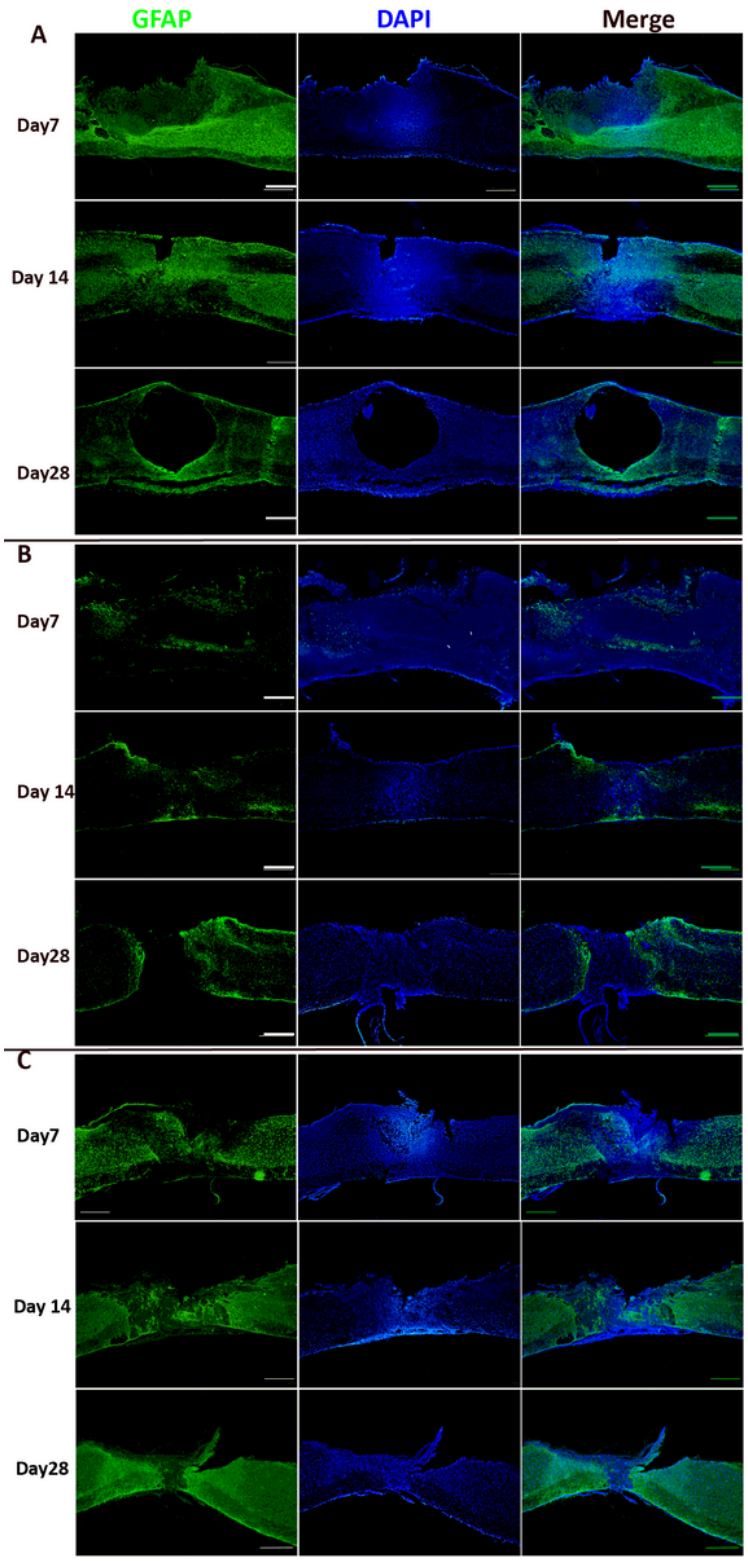

Figure 3

Longitudinal spinal cord sections (14 μm) were immunostained for GFAP to detect astrogliosis. Scale bar: 500 μm.

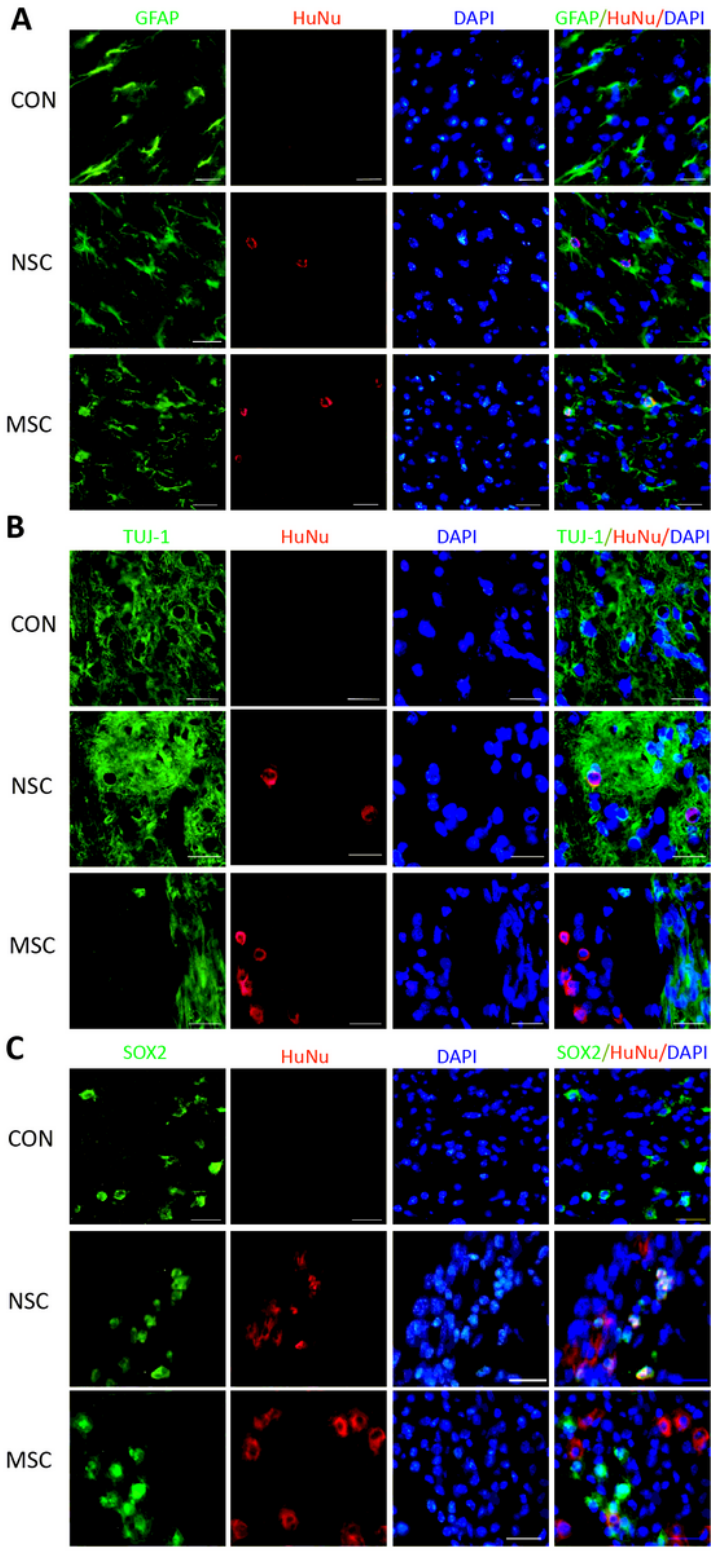

Figure 4

The survival and differentiation of transplanted stem cells. Images of immunofluorescence staining for the GFAP, TUJ-1 and SOX2 markers at dpo 14. Scale bar: 50 μm.

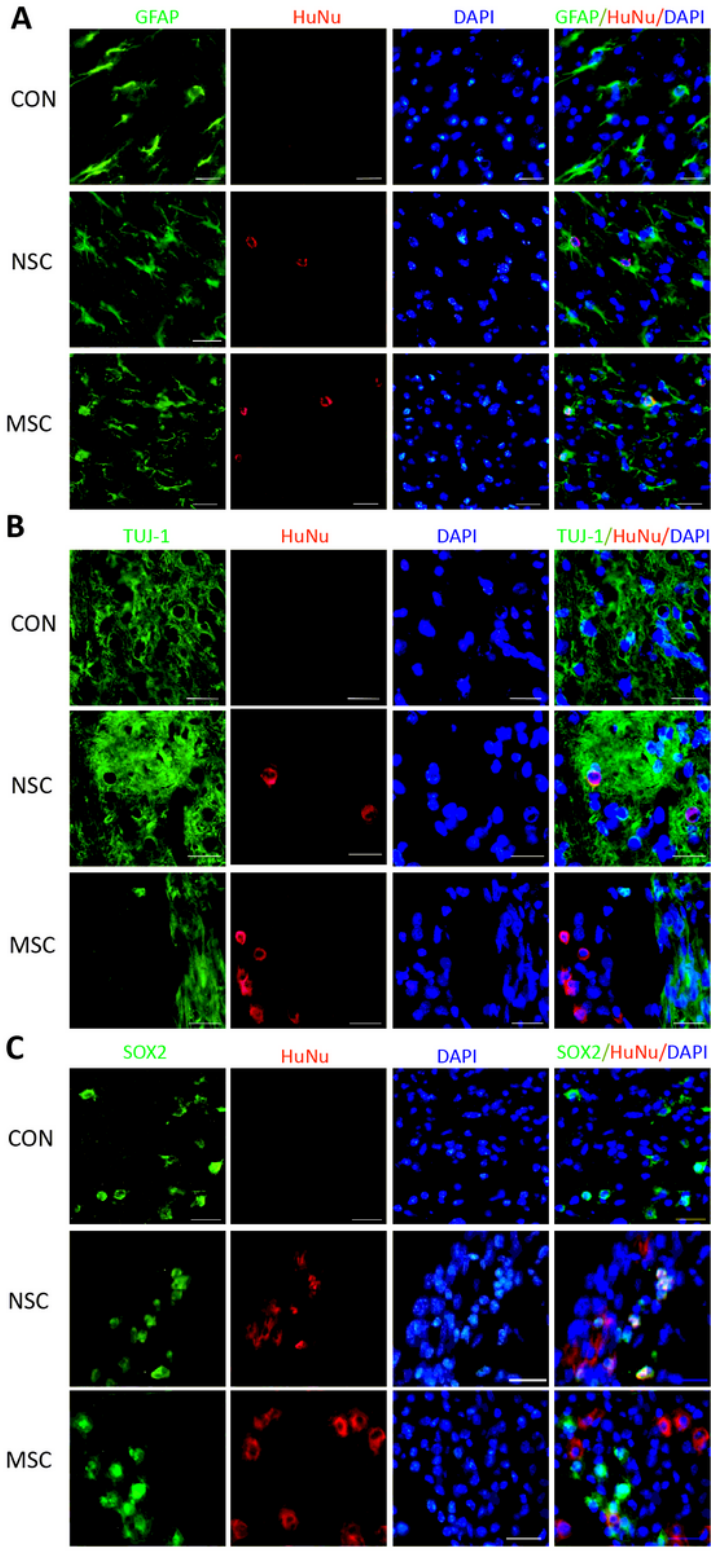

Figure 4

The survival and differentiation of transplanted stem cells. Images of immunofluorescence staining for the GFAP, TUJ-1 and SOX2 markers at dpo 14. Scale bar: 50 μm.

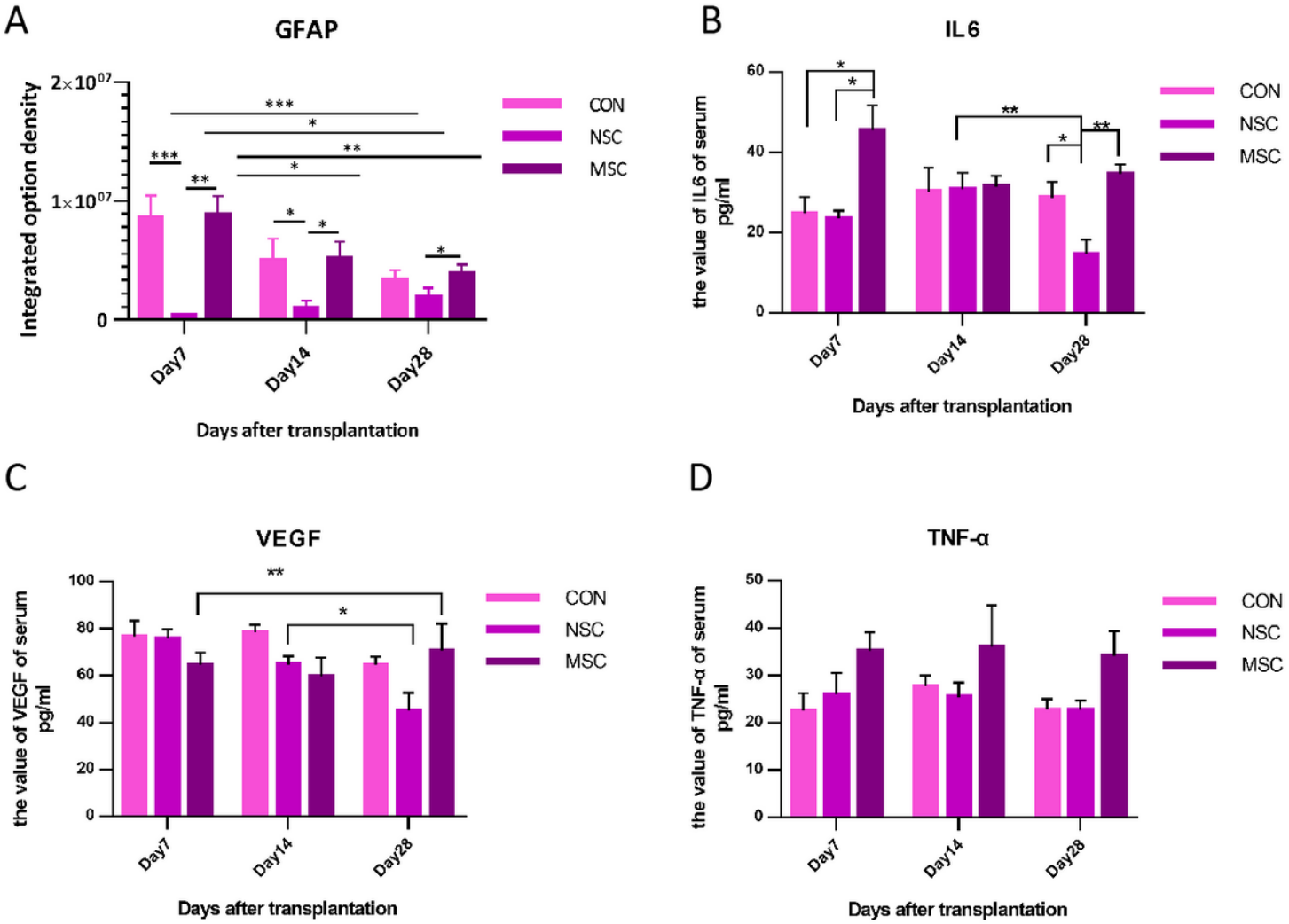

Figure 5

The GFAP expression level in the spinal cord injury site (A) and the serum IL-6 (B), VEGF (C) and TNF-α (D) levels at dpo 7, 14 and 21. All data are presented as the means ± SEM: significance was determined using ANOVA followed by Tukey's post hoc test. *: $p<0.05$; **: $p<0.01$; ***: $p<0.001$.

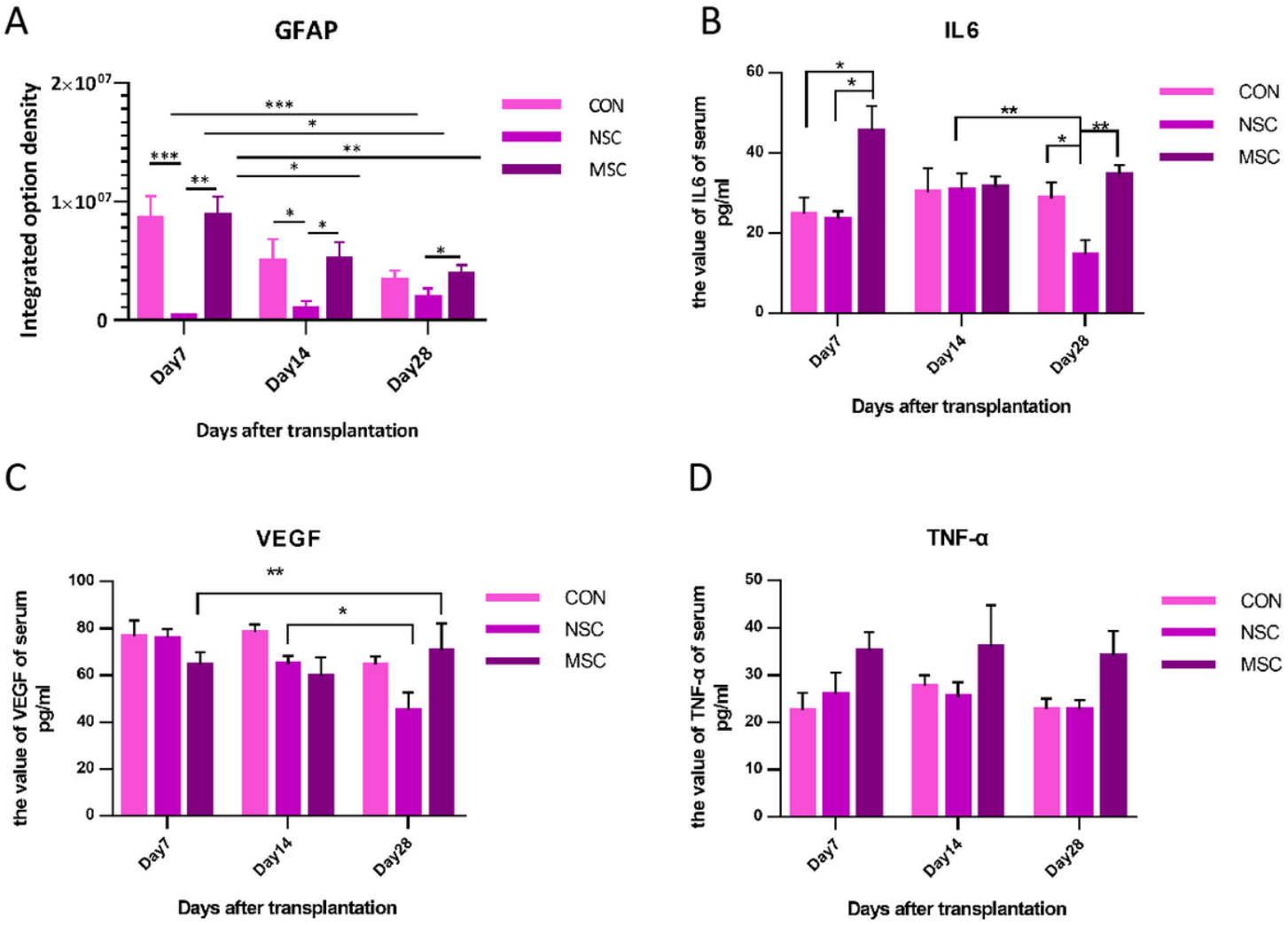

Figure 5

The GFAP expression level in the spinal cord injury site (A) and the serum IL-6 (B), VEGF (C) and TNF-α (D) levels at dpo 7, 14 and 21. All data are presented as the means ± SEM: significance was determined using ANOVA followed by Tukey's post hoc test. *: $p<0.05$; **: $p<0.01$; ***: $p<0.001$.

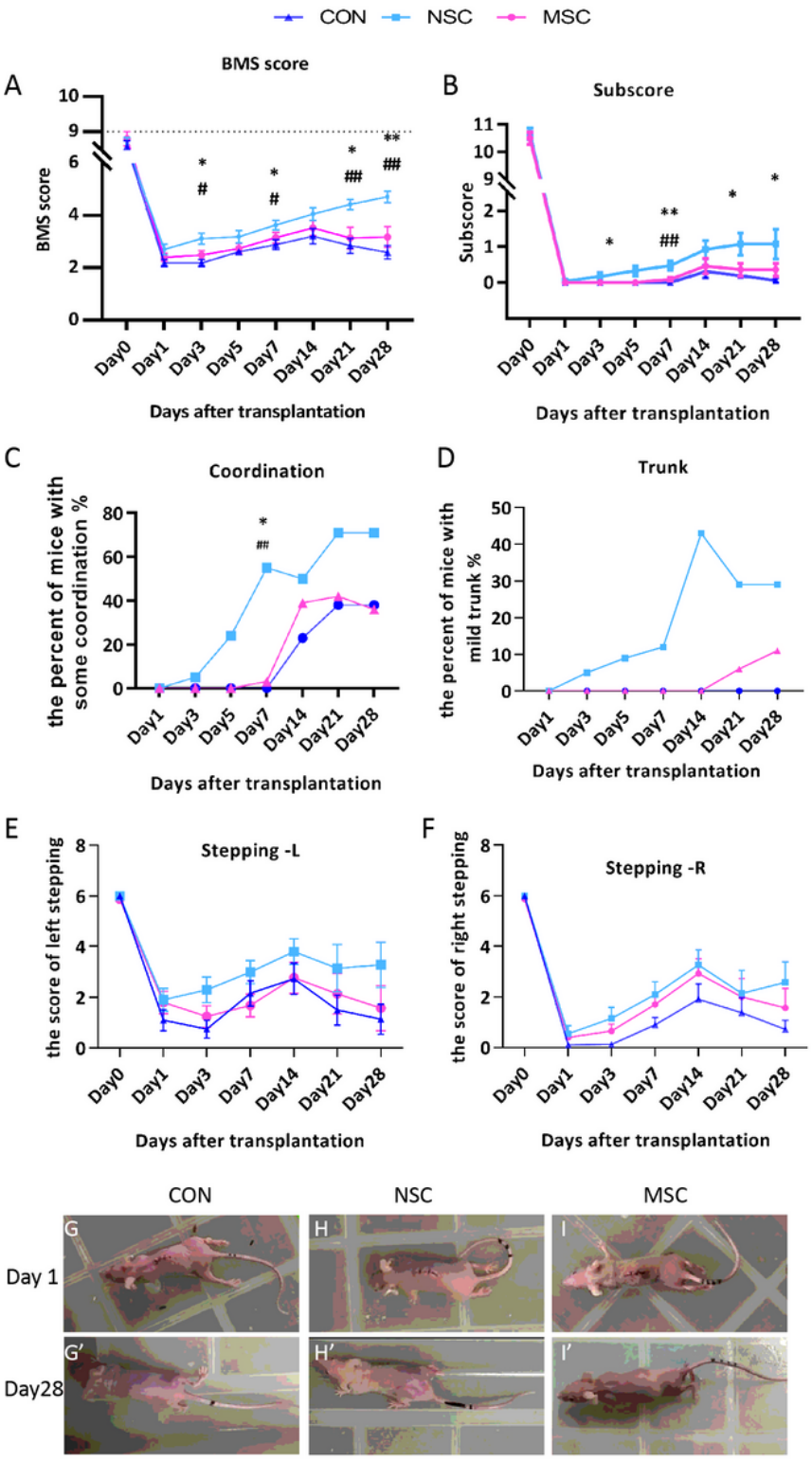

Figure 6

The recovery of locomotor function following stem cell transplantation after SCI. The locomotor function of PBS- or stem cell-treated mice was assessed using the BMS test: BMS score (A), subscore (B), coordination (C), trunk (D), and the stepping score of right side (E) and left side (F). All animals in the NSC group showed significantly higher performance in the open-field BMS test than MSC-treated animals and PBS controls (A). Significantly higher subscores were recorded for the NSC group than the other treatment

groups. Additionally, the MSC-transplanted animals did not show better performance than controls (B). Regarding coordination (C), for which body weight-supported stepping is essential, a stable but insignificant trend of higher performance was observed in the NSC group. The trunk function in the NSC group recovered earlier and to a greater extent than the MSC and control groups (D). A stable but insignificant trend of higher performance on stepping function was observed in the NSC group after the grafting of stem cells (E and F). G-I, Mouse limb function at dpo 1; G'-I', mouse limb function at dpo 28. *: $p < 0.05$ compared with the control group; #: $p < 0.05$ compared with the MSC group.

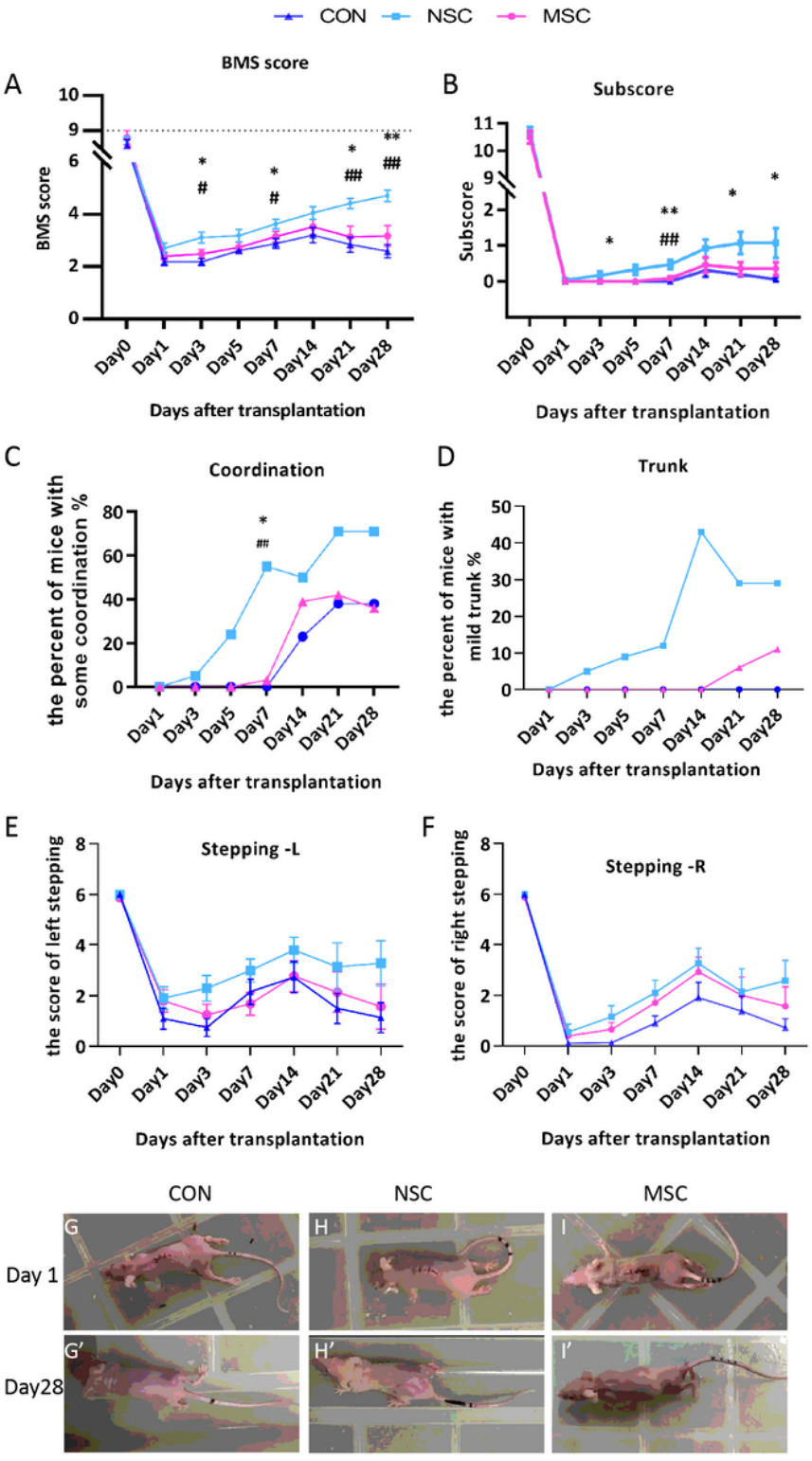

Figure 6

The recovery of locomotor function following stem cell transplantation after SCI. The locomotor function of PBS- or stem cell-treated mice was assessed using the BMS test: BMS score (A), subscore (B), coordination (C), trunk (D), and the stepping score of right side (E) and left side (F). All animals in the NSC group showed significantly higher performance in the open-field BMS test than MSC-treated animals and PBS controls (A). Significantly higher subscores were recorded for the NSC group than the other treatment groups. Additionally, the MSC-transplanted animals did not show better performance than controls (B). Regarding coordination (C), for which body weight-supported stepping is essential, a stable but insignificant trend of higher performance was observed in the NSC group. The trunk function in the NSC group recovered earlier and to a greater extent than the MSC and control groups (D). A stable but insignificant trend of higher performance on stepping function was observed in the NSC group after the grafting of stem cells (E and F). G-I, Mouse limb function at dpo 1; G'-I', mouse limb function at dpo 28. *: $p < 0.05$ compared with the control group; #: $p < 0.05$ compared with the MSC group.

Supplementary Files

This is a list of supplementary files associated with this preprint. Click to download.

- graphicalabstract22.jpg
- graphicalabstract22.jpg
- Table1.doc
- Table1.doc
- Video1.mp4
- Video1.mp4
- video2.mp4
- video2.mp4
- video3.mp4
- video3.mp4
- video4.mp4
- video4.mp4
- video5.mp4
- video5.mp4
- video6.mp4
- video6.mp4